Biochemistry

Article

Aminopyrimidine class aggregation inhibitor effectively blocks A#-fibrinogen interaction and A#-induced contact system activation

Pradeep K. Singh, Masanori Kawasaki, Hanna E. Berk-Rauch, Goushi Nishida, Takeshi Yamasaki, Michael A Foley, Erin H. Norris, Sidney Strickland, Kazuyoshi Aso, and Hyung Jin Ahn

Biochemistry, **Just Accepted Manuscript** • DOI: 10.1021/acs.biochem.7b01214 • Publication Date (Web): 02 Feb 2018

ACS Publications

Biochemistry is published by the American Chemical Society. 1155 Sixteenth Street N.W., Washington, DC 20036

Aminopyrimidine class aggregation inhibitor effectively blocks Aβ-fibrinogen interaction and Aβ-induced contact system activation

Pradeep K. Singh[‡1], Masanori Kawasaki[§&1], Hanna E. Berk-Rauch[‡], Goushi Nishida[§], Takeshi Yamasaki[§], Michael A. Foley[§], Erin H. Norris[‡], Sidney Strickland[‡], Kazuyoshi Aso[§&*], Hyung Jin Ahn[‡*]

[‡]Patricia and John Rosenwald Laboratory of Neurobiology and Genetics, The Rockefeller University, New York, NY 10065, USA; [§]Tri-Institutional Therapeutics Discovery Institute, New York, NY 10021, USA

[*]To whom correspondence should be addressed: Kazuyoshi Aso, 26-1 Muraoka-Higashi 2-Chome, Fujisawa, Kanagawa 255-0012, Japan, Tel: 81-466-32-1121, Fax: 81-466-29-4457; E-mail: kazuyoshi.aso@takeda.com

[*]To whom correspondence should be addressed: Hyung Jin Ahn, 1230 York Avenue New York, NY 10065, USA, Tel: 1-212-327-8773, Fax: 1-212-327-8774; E-mail: hahn@rockefeller.edu

[1]These authors contributed equally.

[&]Present address: Research Division, Chemistry, Axcelead Drug Discovery Partners, Inc., 26-1 Muraoka-Higashi 2-Chome, Fujisawa, Kanagawa 255-0012, Japan

Abstract

Accumulating evidence suggests that fibrinogen, a key protein in the coagulation cascade, plays an important role in circulatory dysfunction in Alzheimer's disease (AD). Previous work has shown that the interaction between fibrinogen and β-amyloid (Aβ), a hallmark pathological protein in AD, induces plasmin-resistant abnormal blood clots, delays fibrinolysis, increases inflammation, and aggravates cognitive function in mouse models of AD. Since Aβ oligomers have a much stronger affinity for fibrinogen than Aβ monomers, we tested whether amyloid aggregation inhibitors could block the Aβ-fibrinogen interaction and found that some Aβ aggregation inhibitors showed moderate inhibitory efficacy against this interaction. We then modified a hit compound so that it not only showed a strong inhibitory efficacy towards the Aβ-fibrinogen interaction but also retained its potency towards the Aβ42 aggregation inhibition process. Furthermore, our best hit compound, TDI-2760, modulated Aβ42-induced contact system activation, a pathological condition observed in some AD patients, in addition to inhibiting the Aβ-fibrinogen interaction and Aβ aggregation. Thus, TDI-2760 has the potential to lessen vascular abnormalities as well as Aβ aggregation-driven pathology in AD.

Introduction

Alzheimer's disease (AD) is a neurodegenerative disorder that leads to profound cognitive decline in the elderly population [1, 2]. AD is a complex, multifactorial disease, and it is likely that various disease mechanisms contribute to pathology [3-5]. Although the direct neuronal toxicity of the AD-related peptide, β-amyloid (Aβ), is well recognized *in vitro*, the precise mechanism by which Aβ disrupts neuronal function in AD patients is unclear [2, 6-8]. Increasing evidence suggests that AD may be a neurological disorder in which circulatory deficiencies significantly contribute to the pathophysiology of the disease [9-14]. Furthermore, it has been shown that Aβ plays an important role in this cerebrovascular dysfunction in AD [15-20]. Therefore, some of the neuronal loss observed in AD patients could be secondary to circulatory problems. For example, many AD patients display altered cerebral blood flow, damaged cerebral vasculature, neuroinflammation, and cerebral microinfarcts [5, 21-24].

Components of the coagulation cascade could contribute to these vascular abnormalities as well as cognitive decline and neurodegeneration in AD [17, 25]. AD patients show increased coagulation factor XII (FXII) activation, kallikrein activity, and high molecular weight kininogen (HK) cleavage in their plasma [17]. Depletion of FXII inhibits HK cleavage as well as reduces neuroinflammation, neurodegeneration, and fibrin(ogen) deposition in the brains of AD mice [25]. Moreover, fibrinogen, the end product of the coagulation cascade, interacts with Aβ with strong affinity, and this interaction increases the aggregation kinetics of Aβ[26]. This interaction also induces abnormal clot structure and increases clot resistance towards fibrinolysis [15, 18, 27, 28]. In addition, fibrinogen is frequently localized to Aβ deposits around the blood vessels of the brain (cerebral amyloid angiopathy, CAA) and the brain parenchyma in AD patients as well as AD mouse models [15, 29-31]. These findings suggest that the Aβ-fibrinogen interaction could be crucial to the onset and progression of neurovascular damage and cognitive impairment in AD. To further support this hypothesis, administration of RU-505, a small compound inhibitor of the Aβ-fibrinogen interaction, reduced cortical inflammation, vascular Aβ deposition, and lessened the severity of cognitive impairment in AD mouse models [27].

The binding affinity of soluble Aβ oligomers to fibrinogen is nearly 10-fold higher than that of Aβ monomers [27]. This finding suggests that minimizing the population of Aβ oligomers could indirectly affect the Aβ-fibrinogen interaction. In addition, several Aβ aggregation inhibitors directly bind Aβ [32, 33], suggesting they may also inhibit the Aβ-fibrinogen interaction directly. Therefore, we screened several known Aβ aggregation inhibitors for the ability to block the Aβ-fibrinogen interaction and found a subset of hits with inhibitor capacity. We then improved the inhibitory efficacy of hit compounds using

medicinal chemistry approaches and found that the best hit compound, TDI-2760, not only showed a strong inhibitory efficacy towards the Aβ-fibrinogen interaction but also modulated Aβ42-induced contact system activation, a pathological condition observed in some AD patients [17].

Materials and Methods

Synthesis of Aβ-aggregation inhibitors. The derivatives of SEN1269 were synthesized as shown in **Scheme 1.**

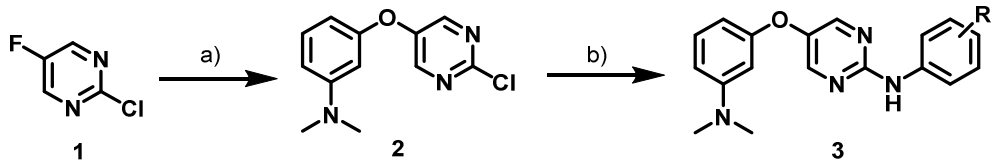

Reagents and conditions: a) K_2CO_3, DMF, 60 °C; b) $ArNH_2$, BrettPhos Pd G3, BrettPhos, *t*-BuOK, DME, 100 °C

Scheme 1. Synthetic scheme of TDI-2760 derivatives.

As described in Scheme 1, 2-chloro-5-fluoropyrimidine (1) was treated with 3-dimethylaminophenol in the presence of K_2CO_3 to afford chloro analog (2). Buchwald amination of (2) using palladium catalyst with various amines worked smoothly to give corresponding amino analogs (3).

Synthesis of 3-(2-Chloropyrimidin-5-yl)oxy-*N*,*N*-dimethyl-aniline. A mixture of 3-(dimethylamino) phenol (11.9 g, 87.1 mmol), 2-chloro-5-fluoro-pyrimidine (15.0 g, 113 mmol, 14.0 mL), and K_2CO_3 (24.1 g, 174 mmol) in DMF (100 mL) was stirred at 60 °C for 48 h. The mixture was quenched with water and diluted with EtOAc. The organic layer was separated, washed with brine, dried over $MgSO_4$, filtered and concentrated in vacuo. The residue was purified by column chromatography (silica-gel, 10-30% EtOAc in hexane) to give the title compound (3.1 g, 12.5 mmol, 14% yield) as an off-white solid; ^{1}H NMR (500 MHz, DMSO-d_6) δ 8.54 (s, 2H), 7.22 (t, J = 8.5 Hz, 1H), 6.58 (d, J = 8.6 Hz, 1H), 6.49 (s, 1H), 6.45 - 6.32 (m, 1H), 2.90 (s, 6H).

General procedure of palladium-catalyzed coupling reaction. A mixture of 3-((2-chloropyrimidin-5-yl)oxy)-*N*,*N*-dimethylaniline (20.0 mg, 80.1 µmol), amine (160 µmol), BrettPhos Pd G3 (7.25 mg, 8.00 µmol), BrettPhos (4.29 mg, 8.00 µmol), KOtBu (27.0 mg, 240 µmol) and DME (1 ml) was heated 100°C for 2 h under microwave irradiation (Synthos 3000, 4x48MC). The reaction mixture was diluted with EtOAc (3 ml), quenched with H_2O (1 ml) and stirred for 2 min. The organic layer was separated, and the aqueous layer was then extracted with EtOAc (2 ml). The combined organic layer was evaporated by

60°C. The residue was purified by preparative HPLC (Actus Triart C18, eluted with MeCN/10mM NH_4HCO_3 aq 5:95 to 100:0). Pure fractions were combined and concentrated by blowing away with the air at 60°C to afford product.

Preparation of Aβ42 solutions. Biotinylated and non-biotinylated synthetic Aβ42 were purchased from Anaspec (Fremont, CA). For AlphaLISA, Aβ42 was reconstituted in a minimal volume of 0.1% NH_4OH and then diluted with 20 mM HEPES buffer (pH 7.4) with 140 mM NaCl. Solubilized Aβ42 was spun at 20,000 x g for 10 min to remove aggregated material and the protein concentration was estimated by BCA (Thermo Scientific). For Aβ42 aggregation studies, monomerized Aβ42 films (Hexafluoro isopropanol, HFIP treated) were prepared as in [34] and diluted in 20 mM Tris-HCl (pH 7.4) or 20 mM HEPES buffer (pH 7.4) with 140 mM NaCl. Aβ42 oligomers were prepared as described in [34]. Briefly, monomerized Aβ42 films were reconstituted in DMSO by sonication for 10 min and incubated overnight with slow agitation (40 rpm) at 4°C either in 20 mM Tris-HCl (pH 7.4) or 20 mM HEPES buffer (pH 7.4) with 140 mM NaCl. After, overnight incubation, the solution was centrifuged at 20,000 x g for 10 min. The protein concentration was estimated by Pierce BCA protein assay kit (Thermo Scientific).

AlphaLISA. Various concentrations (0. 1 – 100 μM) of compounds were plated in white 384-well plates (Greiner) and were incubated with 10 nM biotinylated Aβ42 (Anaspec) and 1 nM fibrinogen for 30 min at room temperature (RT) in a final volume of 10 μl assay buffer (25 mM Tris-HCl, pH 7.4, 150 mM NaCl, 0.05% Tween-20, and 0.1% BSA). The mixture was then incubated with anti–fibrinogen antibody (Dako), 20 μg/ml streptavidin-conjugated donor, and protein A–conjugated acceptor beads (PerkinElmer) for 90 min at RT. Samples were read by a PerkinElmer EnVision plate reader. RU-505, which is a known inhibitor of Aβ42-fibrinogen interaction[27], was used as a positive control and also for comparison of its efficacy with other compounds. All the experiments were performed in triplicate. To determine IC_{50} of compounds, the data were fitted to a sigmoidal dose-response equation (Y= Bottom + (Top – Bottom)/1 + $10^{(\log IC50 - X)\cdot \text{Hill coefficient})}$) using GraphPad Prism 4 to calculate IC_{50}.

***In vitro* clotting (turbidity) assay.** Turbidity assays were performed at RT in high binding 96-well plates (Fisher Scientific) in triplicate using a Spectramax Plus384 reader (Molecular Devices). For *in vitro* fibrin clot formation, fibrinogen (1.5 μM) with or without Aβ42 oligomers (3 μM) was mixed with thrombin (0.5 U/mL) and $CaCl_2$ (5 mM) in 20 mM HEPES buffer (pH 7.4) with 137 mM NaCl in a volume of 200μl. To test the efficacy of SEN1269 and its analogs in restoring the Aβ42-induced reduction in clot

turbidity, clot formation was also initiated in the presence of these compounds (20 μM) with Aβ42 oligomers (3μM). The effect of these compounds was also tested in normal fibrin clotting experiments without adding Aβ42 oligomers. Clot formation was monitored by measuring the change in turbidity at 450 nm over time.

Monitoring Aβ42 aggregation kinetics. Monomerized Aβ42 films (Hexafluoro isopropanol, HFIP, treated) were reconstituted in DMSO by sonication as in [34]. The solution was then diluted in 20 mM HEPES buffer (pH 7.4) with 140 mM NaCl and centrifuged at 14,000 rpm at 4°C for 10 min to remove any aggregated species. The supernatant was collected, and Aβ42 concentration was estimated using the BCA method for protein quantification. The Aβ42 solution was kept on the ice and used for aggregation study reaction setup within 30 min. For amyloid aggregation kinetics, we used 96-well flat bottom microtiter black plates (Greiner), and the Aβ42 solution was added to the wells in the presence or absence of compounds. The final concentration of Aβ42 was 12.5 μM, and the final concentration of compounds was 48 μM in a total reaction mixture of 150 μl. Because the stock solutions of these compounds were in DMSO, the equivalent residual DMSO concentration was also added to Aβ42 alone solution. To monitor the time dependent Aβ amyloid assembly, ThT dye [35] was added to each well to a final concentration of 33 μM in the solution. Buffer alone in the presence and absence of compounds was also used with ThT as controls. The plate was sealed with an adhesive film (Thin Seal) and incubated at 37°C with a shaking speed of 25 rpm (Environ Orbital Shaker). Time dependent ThT fluorescence was recorded (once an hour) by quickly taking out the microtiter plate from the shaker and directly measuring the emission maxima at 480 nm with an excitation wavelength of 440 nm, using a Spectramax M2e plate reader (Molecular Devices). The microtiter plate was sealed after every measurement and incubated at 37°C for a total of 26 hrs. All the experiments were performed in triplicate.

Scanning electron microscopy (SEM). Fibrin clots were formed using purified human fibrinogen (Calbiochem) on round glass coverslips at RT. Fibrin clots in the presence or absence of oligomeric Aβ42 were formed as described above for the turbidity assay. To test the efficacy of SEN1269 and its analogs, these compounds (20 μM) or DMSO were preincubated with Aβ42 oligomers (3.0 μM) for 10 mins with slow shaking at RT. Fibrinogen (1.5 μM) was added into compound-Aβ42 mixtures, and the reaction was initiated by adding thrombin (0.5 U/mL). Thirty mins after adding thrombin, clots were gently washed twice with cold sodium cacodylate buffer (0.1M; 2 min each) and fixed with 2% glutaraldehyde (on ice for 30 min). After serial dehydration by ice cold ethanol (20-100%), dried fibrin clots were sputter-coated

with gold palladium. Images were obtained using a LEO 1550 scanning electron microscope at the Electron Microscopy Resource Center at The Rockefeller University.

Transmission electron microscopy (TEM). For visualizing the morphology of Aβ42 aggregates in the presence and absence of hit compounds, after 26 hrs of incubation, the undiluted Aβ42 (12.5 μM) samples (in the presence and absence of compounds) were applied to glow-discharged CF200-Cu grids (Electron Microscopy Sciences), washed three times with ultrapure water, negatively stained with 2% uranyl acetate, and air-dried. Electron micrographs were acquired using the FEI TECNAI G2 Spirit BioTwin transmission electron microscope (120 Kv) equipped with Gatan 4K x 4K digital camera in Electron Microscopy Resource Center at The Rockefeller University.

Kallikrein activity assay. To test the effect of TDI-2760 on Aβ42 oligomer-induced kallikrein generation *in vitro*, Aβ42 oligomers in the presence or absence of TDI-2760 were incubated in 20 mM HEPES buffer (pH 7.4) with 140 mM NaCl in a 96-well microtiter plate (Fisher Scientific). The plate was sealed with an adhesive sealing film (Thin Seal) and incubated at RT with a shaking speed of 25 rpm for 30 min. Buffer (in the presence or absence of TDI-2760) without Aβ42 oligomers was also incubated. After 30 min, 10 nM of purified human coagulation factor XII (FXII; Haematologic Technologies Inc) and 10 nM of human plasma prekallikrein (PPK; Enzyme Research Laboratories) were added to each well. Finally, chromogenic substrate S-2302^{TM} (Chromogenix) was added to each well to a final concentration of 0.67 mM in a 100 μl reaction mixture. Time dependent change in the absorbance was recorded by measuring the absorbance at 405 nm at RT with a Spectramax Plus 384 reader (Molecular Devices). In the reaction mixture of 100 μl, the final concentration of Aβ42 oligomer was 1μM and TDI-2760 was 40 μM. Experiments were performed in triplicate, and dextran sulfate (DXS) (0.1 μg/ml) was used as a positive control. DXS (0.1 μg/ml) in the presence of TDI-2760 (40 μM) was also used to check the specificity of TDI-2760. The rate of substrate (S-2302^{TM}) conversion over time (30 min) was also calculated for each sample by Softmax 6.1 (Molecular Devices) and represented as milli-units per min.

Statistical analysis. All numerical values presented in graphs are mean ± SEM. Statistical significance in Figure 5 was determined using Student's two-tailed t-test. For all the AlphaLISA IC_{50} analyses, 95% confidence interval (95% CI) was used as the statistical parameter.

Results

Some Aβ aggregation inhibitors can block the Aβ-fibrinogen interaction. Biochemical analysis using AlphaLISA showed that the binding affinity of soluble Aβ oligomers to fibrinogen is nearly 10-fold higher than that of Aβ monomers [27]. Therefore, we hypothesized that Aβ aggregation inhibitors may indirectly minimize the Aβ-fibrinogen interaction by decreasing Aβ oligomerization. In addition, we hypothesized that some Aβ aggregation inhibitors may directly bind to Aβ [32, 33] and disrupt the Aβ-fibrinogen interaction directly. Based on these hypotheses, we synthesized and evaluated a series of known Aβ aggregation inhibitors/β-sheet breakers [32, 36-42] for their efficacy against the Aβ-fibrinogen interaction using AlphaLISA (Table 1). Some of the β-sheet breakers possessed efficacy against the fibrinogen-Aβ interaction (IC_{50} values are shown in Table 1). However, the efficacy of these compounds (IC_{50}) varied considerably. For example, RS-0406, SEN1576, and tanshinone [36, 41, 42] showed almost no efficacy (IC_{50} > 100 μM), whereas SEN1269 [32] showed the best efficacy in blocking the Aβ42-fibrinogen interaction (IC_{50} = 17.8 μM). Since SEN1269 has the highest inhibitory efficacy, we selected this compound for structure activity relationship (SAR) study.

Chemical modification of SEN1269 to improve its inhibitory efficacy against the Aβ42-fibrinogen interaction. To improve the potency of SEN1269, we modified the chemical structure of the SEN1269 scaffold. SAR of the right-hand side (RHS) of SEN1269 is summarized in Table 2. The inhibitory activity of SEN1269 analogs against the Aβ42-fibrinogen interaction was determined using AlphaLISA, and IC_{50} values were calculated (Table 2). The methoxy analogs (Table 2; TDI-2758 Entry 2, TDI-3066 Entry 3, and TDI-3067 Entry 4) were evaluated, and it was found that the substituent in the *meta* position (TDI-2758) was most effective among the three analogs (IC_{50} = 6.42 μM for Entry 2 vs IC_{50} = 25.0 and 29.0 μM, for Entry 3 and 4, respectively). Compared to the parent molecule, the substituents in the *ortho* and *para* positions actually led to decreased inhibitory activity against the Aβ42-fibrinogen interaction. Furthermore, the phenyl analog (TDI-2760; Table 2 Entry 6 and Figure 1A) showed much higher efficacy against this interaction (IC_{50} = 1.67 μM) in AlphaLISA (Table 2 and Figure 1B). In comparison to its parent molecule, the inhibitory efficacy (IC_{50}) of TDI-2760 was increased ~ 10-fold (17.8 μM vs 1.67 μM). RU-505 is a known inhibitor of the Aβ42-fibrinogen interaction[27], and thus we included it in our study as a positive control (Figure 1).

Next, a SAR study of the left hand side (LHS) was also conducted (Table S1). The dimethylamino substituent on the phenyl group was crucial to disrupt the interaction (Table S1; Entry 1 and 2), and the

pyrrolidine analog, TDI-3222, led to enhanced activity (Table S1; Entry 5; IC_{50} = 3.12 μM). This result would suggest that an electron-donating amino group leads to enhanced potency. To test this hypothesis, difluoropyrrolidine analog TDI-3906 was evaluated and revealed a decreased potency (Table S1; Entry 6; IC_{50} = 88.3 μM). In addition, we tested several other LHS analogs including morpholino and mono-N-methyl analog, but only the N-methyl analog led to improved potency effectively compared with the original compound (Table S1; Entry 10, IC_{50} = 3.76). Based on these preliminary SAR results, we found that TDI-3222 and TDI-3256, which were obtained by LHS modifications, have better inhibitory efficacy against the Aβ42-fibrinogen interaction (IC_{50} = 3.12 μM and 3.76 μM, respectively). Overall, the TDI-2760, which was obtained by RHS modifications exhibited the most potent efficacy against the Aβ42-fibrinogen interaction as its IC_{50} value was 10-fold lower than its parent molecule, SEN1269 (1.67 μM vs 17.8 μM, respectively).

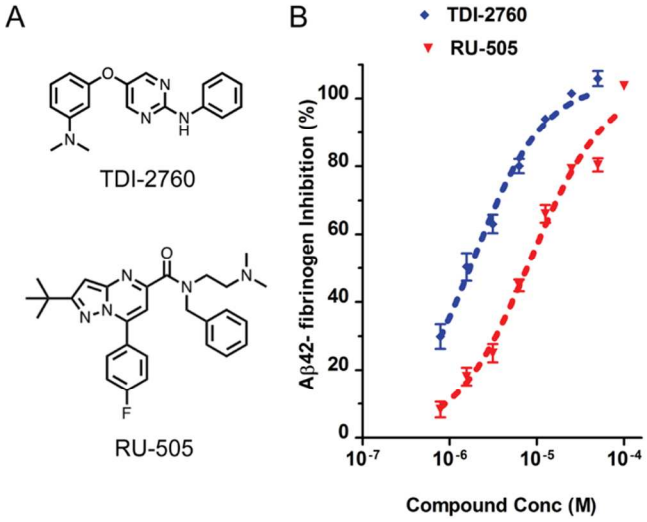

Figure 1. TDI-2760 blocks the interaction between Aβ42 and fibrinogen in AlphaLISA. (A) The chemical structures of TDI-2760 and RU-505. (B) Representative AlphaLISA reading, showing the effect of TDI-2760 on the Aβ42-fibrinogen interaction. IC_{50} of TDI-2760 was determined, and RU-505 was used as a positive control since it inhibits the Aβ42-fibrinogen interaction. The experiment was performed in triplicate, and mean ± SEM values were plotted. Blue = TDI-2760; Red = RU-505.

Validating the inhibitory efficacy of SEN1269 and its analogs against the Aβ42–fibrinogen interaction using an *in vitro* clotting assay. As the interaction between fibrinogen and Aβ induces a structurally abnormal fibrin clot [15, 18, 27], we tested whether SEN1269 and its analogs (TDI-3222, TDI-3256, and TDI-2760) can restore Aβ-induced altered thrombosis *in vitro*. We also included TDI-2758 (Entry 2, Table 2) in the assays, since this analog also showed improved inhibitory efficacy against the Aβ-fibrinogen interaction by AlphaLISA.

During clot formation, fibrinogen molecules are cleaved by thrombin and associate into a fibrin network, which scatters light and causes the solution to increase in turbidity. Thus, the kinetics of turbidity can be

used as a read-out to examine fibrin clot formation[27]. Each compound (20 μM) or vehicle (0.4% DMSO) was incubated with purified human fibrinogen in the presence or absence of oligomeric Aβ42. Fibrin clot formation was analyzed by measuring the turbidity immediately after adding thrombin to the mixture. The maximum turbidity of the fibrin clot decreased in the presence of Aβ42, since it alters fibrin clot structure (Figure 2A-D). In the *in vitro* clotting assay, SEN1269 further decreased the turbidity of the clot formed in the presence or absence of Aβ42 (Figure 2A). This result indicates that SEN1269 also altered normal fibrin clot structure, which was undesirable. In contrast, TDI-2758 and TDI-3256 did not alter the turbidity of the normal fibrin clot formed in the absence of Aβ42 (Figure 2B and 2C, green), but clot turbidity was further decreased in the presence of both Aβ42 and TDI-2758/TDI-3256 (Figure 2B and 2C, purple). This result was the opposite of what we expected, as these analogs showed an inhibitory effect on the Aβ42-fibrinogen interaction in AlphaLISA. TDI-3222 did not show any effect in the turbidity assay due to its color causing a high background (data not shown).

In contrast to the other compounds, phenyl analog TDI-2760 was very effective in the turbidity assay as it partially restored the Aβ42-induced abnormal fibrin clot formation (Figure 2D, purple vs red). Additionally, TDI-2760 did not alter the turbidity of the normal clot in the absence of Aβ42 (Figure 2D, green vs blue). This observation indicates that TDI-2760 specifically restores the Aβ-induced decrease in turbidity during fibrin clot formation without affecting normal thrombosis. In conclusion, TDI-2760 effectively inhibits the Aβ-fibrinogen interaction and partially restores Aβ42-induced abnormal fibrin clot formation.

The results of the turbidity assay were further validated by analyzing *in vitro* fibrin clots using scanning electron microscopy (SEM). Fibrin clots were prepared from purified fibrinogen in the presence of $CaCl_2$ and thrombin, and SEM images of fibrin clots showed a typical three-dimensional mesh of elongated fibrin threads (Figure 3A). However, in the presence of Aβ42 oligomers, the fibrin threads were relatively thinner (Figure 3B) and several clumped structures were observed, indicating that the architecture of the fibrin clot was altered in the presence of Aβ42 (Figure 3B). Consistent with the turbidity assay, TDI-2760 partially restored the Aβ42-induced abnormal fibrin clot structure as evidenced by fewer clumps and relatively thicker fibrin threads under SEM (Figure 3C). However, the SEM analysis of fibrin clots in the presence of Aβ42 and SEN1269 (Figure 3D) or TDI-2758 (Figure 3E) suggested that SEN1269 and TDI-2758 failed to restore the Aβ42-induced clot abnormality. In fact, clots formed in the presence of Aβ42 with SEN1269 or TDI-2758 showed more clumps and compromised clot architecture more severely than

clots formed in the presence of Aβ42 oligomers only (Figure 3D and 3E). This finding was consistent with the results obtained from the turbidity assay, in which SEN1269 and TDI-2758 further decreased the turbidity of the fibrin clots formed in the presence of Aβ42 (Figure 2A and 2B).

Even though TDI-2760 did not affect normal thrombosis in the turbidity assay (Figure 2D), we further tested whether TDI-2760 affects thrombin proteolytic activity or blood coagulation, using a chromogenic substrate assay and activated partial thromboplastin time (aPTT) test, respectively. Our assay results showed that TDI-2760 did not alter the activity of thrombin in the chromogenic substrate assay (Figure S1) and did not have any effect on the coagulation profile of human pooled normal plasma in a microtiter plate based-aPTT test (Figure S2).

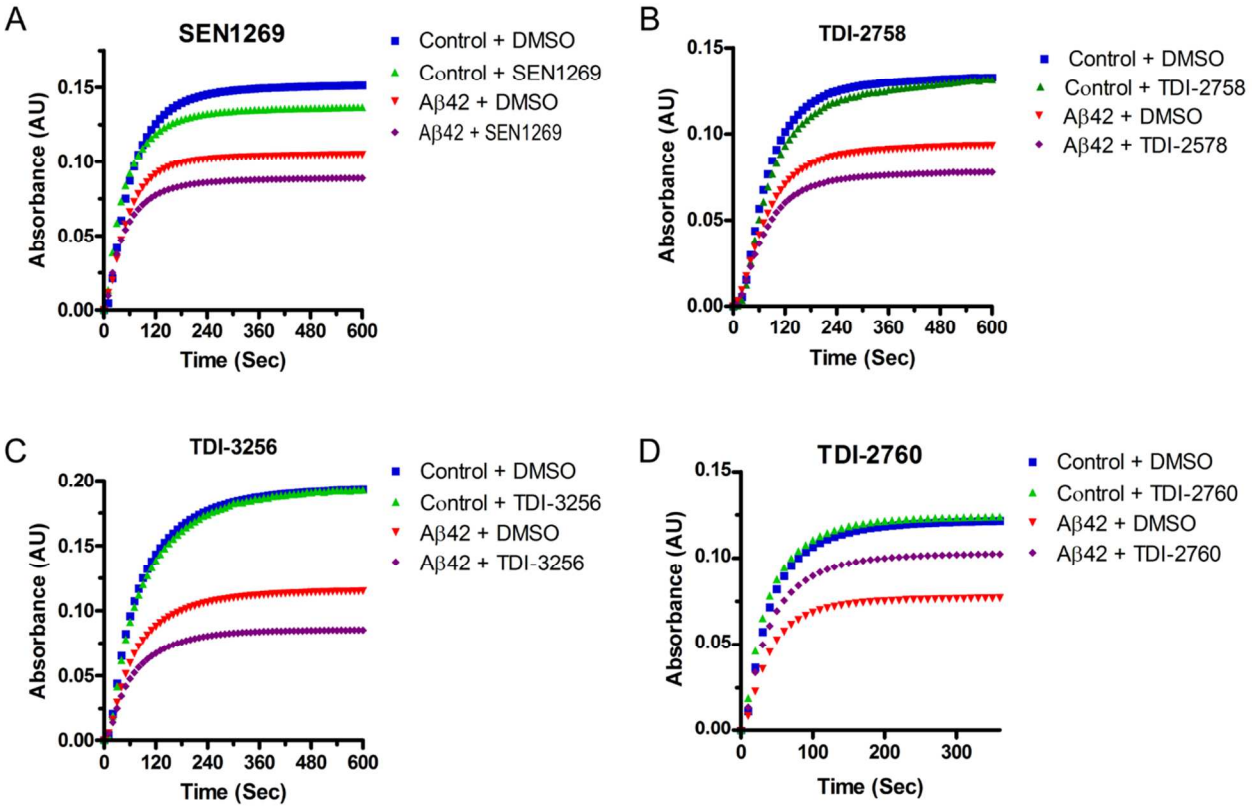

Figure 2. TDI-2760 restores the Aβ42-induced decrease in fibrin clot turbidity without affecting normal clotting in an *in vitro* clotting assay. Individual test compounds or DMSO (vehicle) were incubated with fibrinogen in the presence or absence of Aβ42 (3 μM), followed by addition of thrombin and $CaCl_2$. Fibrin clot formation was assessed by measuring time-dependent turbidity changes at 450 nm (n = 3 experiments/compound). (A) SEN1269 decreased the clot turbidity of the normal clot formed in the absence of Aβ42 (green vs blue) as well as the turbidity of the clot formed in the presence of Aβ42 (purple vs red). (B) In the presence of TDI-2758, the turbidity of clots formed with Aβ42 was decreased

(purple vs red). (C) In the presence of TDI-3256, the turbidity of clots formed with Aβ42 was also decreased (purple vs red). (D) TDI-2760 did not alter the turbidity of the normal clot (blue vs green) but restored the Aβ42-induced decrease in turbidity during fibrin clot formation (purple vs red).

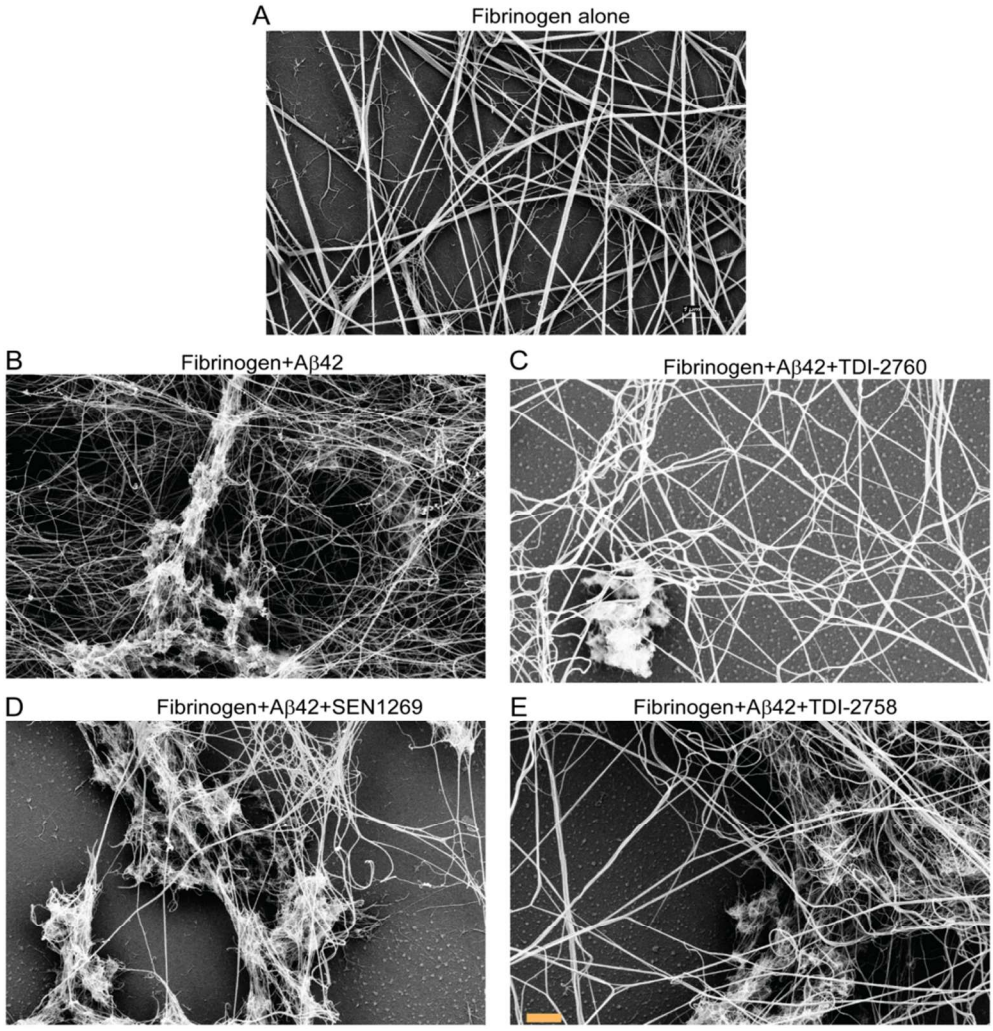

Figure 3. SEM analysis of the effect of hit compounds on Aβ42-induced abnormal fibrin clot structure. Individual compounds (20 μM) or DMSO (vehicle) were incubated with fibrinogen (1.5 μM) in the presence or absence of Aβ42 oligomers (3 μM), and clot formation was initiated by adding thrombin into the mixture. Fibrin clot structures were analyzed by SEM. SEM images of clots formed by (A) Fibrinogen alone, (B) Fibrinogen+Aβ42, (C) Fibrinogen+Aβ42+TDI-2760, (D) Fibrinogen+Aβ42+SEN1269, (E) Fibrinogen+Aβ42+TDI-2758. SEM analysis revealed that Aβ42 oligomers altered the fibrin clot structure, and TDI-2760 partially restored the Aβ42-induced structural abnormality of fibrin clot while SEN1269 and TDI-2758 did not. Scale bar is 1 μm.

TDI-2760 effectively inhibits Aβ42 aggregation. SEN1269 was not effective in reversing the Aβ42-induced decrease in clot turbidity and altered clot structure (Figure 2A and Figure 3D). However, SEN1269 has been shown to be a potent Aβ aggregation inhibitor[32], and it also effectively inhibited Aβ42 aggregation in our study (Figure S3). Therefore, we investigated if SEN1269 phenyl analog, TDI-2760, also retained this inhibitory efficacy towards Aβ42 aggregation *in vitro*. The time-dependent Aβ42 aggregation kinetics were probed using an amyloid-specific dye, thioflavin T (ThT)[35]. The typical amyloid aggregation process (when probed using ThT) shows a sigmoidal growth curve with lag phase, log phase, and stationary phase. The stationary phase (with a plateau), usually represents the completion of the amyloid fibrillization process[43]. The ThT fluorescence of Aβ42 (12.5 μM) in the presence and absence of TDI-2760 (48 μM) was recorded at different time intervals. The ThT fluorescence data of Aβ42 alone showed a typical sigmoidal curve, characteristic of the amyloid aggregation pathway (red in Figure 4A).

In contrast, Aβ42 in the presence of TDI-2760 did not show such characteristics and the ThT fluorescence was significantly lower (blue in Figure 4A). This result indicates minimal Aβ42 amyloid fibril formation in the presence of TDI-2760. ThT fluorescence of buffer in the presence and absence of TDI-2760 without Aβ42 addition remained low during the incubation period (data not shown). To confirm this result, we used transmission electron microscopy (TEM) to examine the end products of Aβ42 aggregation in the presence or absence of TDI-2760 after 26 hrs incubation. TEM of Aβ42 showed mainly fibrillar structures with few oligomers (Figure 4B), consistent with high ThT fluorescence (Figure 4A). However, TEM of Aβ42 in the presence of TDI-2760 showed very few fibrillar structures (Figure 4C), consistent with low ThT fluorescence (Figure 4A). The ThT fluorescence data and TEM analysis clearly revealed that TDI-2760 effectively inhibits Aβ42 aggregation. This observation suggests that removing the hydroxyl (-OH) group improves the inhibitory efficacy of SEN1269 against the Aβ42-fibrinogen interaction without diminishing its ability to inhibit Aβ42 aggregation.

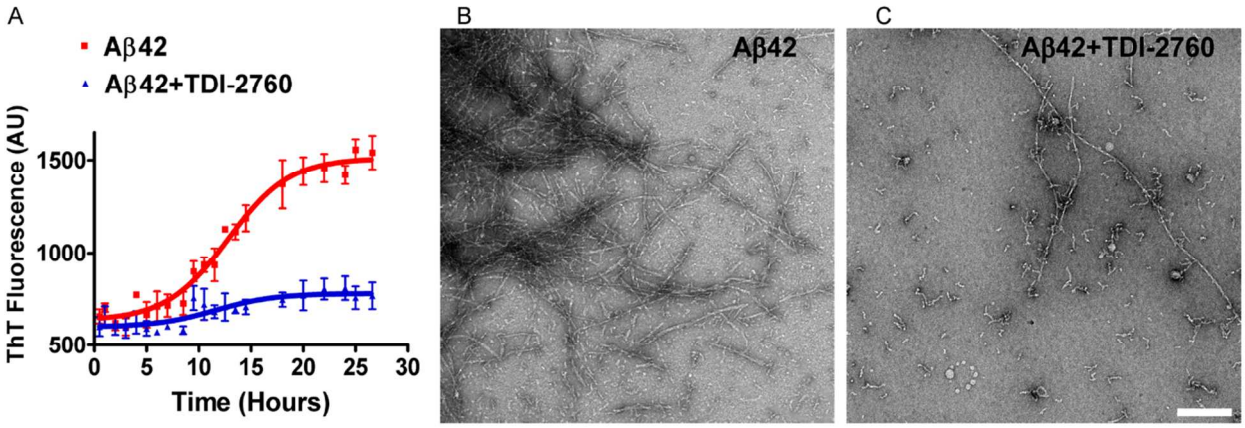

Figure 4. TDI-2760 inhibits Aβ42 fibrillization. Aβ42 aggregation in the presence and absence of TDI-2760 was examined by monitoring amyloid aggregation kinetics by ThT fluorescence. (A) ThT fluorescence was monitored over time by measuring the emission maxima at 480 nm, with an excitation wavelength of 440 nm. ThT fluorescence of the Aβ42 alone (red) showed a time-dependent increase and displayed a sigmoidal growth curve, which is a typical characteristic of amyloid aggregation. In the presence of TDI-2760 (blue), the Aβ42-induced time-dependent increase of ThT fluorescence was significantly reduced, suggesting that TDI-2760 strongly inhibits Aβ42 fibrillization. The experiment was performed in triplicate, and the graph is presented as mean± SEM value. (B, C) After 26 hrs, these samples were visualized by TEM. TEM images of Aβ42 alone (B) showed predominately fibrillar species along with some oligomers. The fibrillar and oligomeric species of Aβ42, however, were substantially decreased in the presence of TDI-2760 (C), suggesting the inhibitory efficacy of this compound against Aβ42 aggregation. Scale bar is 100 nm.

Effect of TDI-2760 on Aβ42-mediated initiation of contact activation system. Induction of the coagulation factor XII (FXII)-driven contact activation pathway can be initiated by Aβ42 [17, 44-47], leading to cleavage of coagulation factor XI (FXI) and blood clotting and activation of plasma prekallikrein (PPK) and release of bradykinin from high molecular weight kininogen (HK) [48]. This activation could play a role in the vascular and inflammatory aspects of AD pathology by launching both prothrombotic and proinflammatory pathways [25]. Since SEN1269 binds to Aβ42 in a surface plasmon resonance experiment [32], TDI-2760, the phenyl analog of SEN1269, may bind to Aβ42, since it showed strong inhibition against the Aβ42 aggregation process (Figure 4). We speculated that if TDI-2760 interacts with Aβ42, it may also affect Aβ's activation of FXII and subsequent cleavage of FXI to FXIa and/or PPK to kallikrein. To test this hypothesis, we measured the *in vitro* kallikrein activity using purified human coagulation components (FXII and PPK) and a chromogenic substrate, S-2302™. Aβ42 oligomers in the presence and absence of TDI-2760 were tested for their potential to activate FXII and thus produce kallikrein. Kallikrein then can cleave its chromogenic substrate S-2302™ which can be quantified by

measuring absorbance at 405 nm [17]. Aβ42 oligomers (1μM) showed high kallikrein activity in the reaction mixture of purified coagulation components and the S-2302™ substrate, as indicated by high absorbance at 405 nm (red in Figure 5A).

However, Aβ42 oligomers incubated in the presence of TDI-2760 (40 μM) showed significantly less absorbance at 405 nm compared to Aβ42 oligomers alone (blue in Figure 5A). The buffer in the presence and absence of TDI-2760 (40 μM) without Aβ42 addition showed insignificant kallikrein activity (purple and green in Figure 5A). This suggests that binding of TDI-2760 to Aβ42 oligomers lessens the ability of Aβ to induce FXII activation and its subsequent generation of kallikrein. Consistent with this result, the rate of S-2302™ substrate conversion was also significantly lower in the Aβ42 oligomers incubated with TDI-2760 sample (22.06±0.73 vs 10.06±0.78 milli-units per min, respectively) (Figure 5B). Dextran sulfate (DXS, MW 500, KDa) [17] was used as a positive control and showed high kallikrein activity (red in Figure 5C). Additionally, TDI-2760 (40 μM) did not alter the kallikrein activity induced by DXS (0.1 μg/ml) (blue in Figure 5C), indicating the specificity of TDI-2760 towards Aβ42. These data suggest that TDI-2760 is effective at blocking the Aβ42-induced activation of the FXII-mediated contact system.

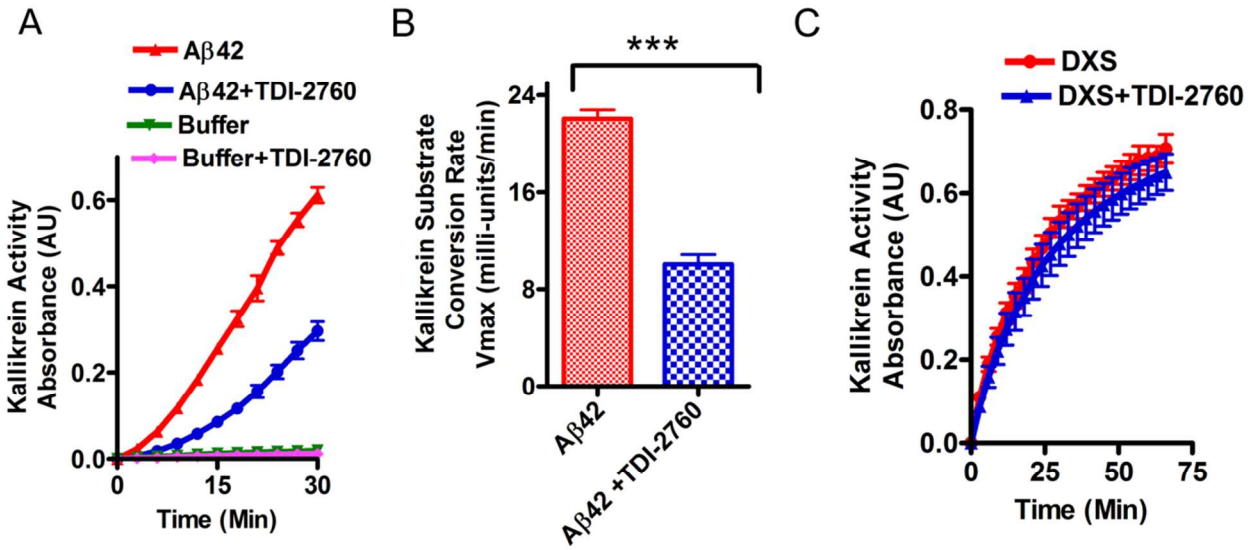

Figure 5. Effect of TDI-2760 on Aβ42-mediated contact activation. (A) Purified human coagulation factor XII (FXII) and human plasma prekallikrein (PPK) were used in the assay, and kallikrein activity was triggered by adding Aβ42 oligomers incubated in the presence or absence of TDI-2760. The final concentration of Aβ42 oligomers was 1 μM and TDI-2760 was 40 μM in the reaction. Buffer alone (green) and buffer with TDI-2760 (purple) showed essentially no kallikrein activity. Aβ42 alone (red) significantly increased kallikrein activity, while TDI-2760 with Aβ42 (blue) led to a significant decrease in the amount of kallikrein release. (B) Vmax was calculated from the assay in (A). Pre-incubating TDI-2760 to Aβ42 oligomers prior to this assay led to a significantly lower substrate (S-2302™) conversion

rate (Vmax) ($p<0.001$). The experiment was performed in triplicate, and mean ± SEM values are plotted. (C) Dextran sulfate (DXS, red, 0.1 μg/ml), a positive control for kallikrein activation, was not influenced by pre-incubation with TDI-2760 (blue, 40 μM), indicating TDI-2760's specificity for Aβ42. Statistical significance was determined by non-parametric unpaired (two-tailed) t- test. $p \leq 0.001$ was designated as (***).

Discussion

Several studies indicate that Aβ aggregation initiates a cascade of molecular events, eventually leading to neuronal death and dementia in AD [1, 2, 6-8]. Therefore, targeting Aβ aggregation has increasingly become a focus of a potential therapeutic approach for AD [32, 33, 38, 49-54]. Despite tremendous efforts, drug development of Aβ aggregation inhibitors has proven very difficult and the results of ongoing clinical trials of those inhibitors are mostly inconclusive [55, 56]. In this study, we have shown that some Aβ aggregation inhibitors [32, 36-40] have the intrinsic ability to disrupt the Aβ-fibrinogen interaction (Table 1). These characteristics together would be beneficial not only in altering Aβ aggregation-related toxicity, but also in modulating vascular abnormalities that arise from the Aβ-fibrinogen interaction in AD.

Because our previous work indicated that Aβ oligomers have stronger affinity for fibrinogen than monomers, we tested whether Aβ aggregation inhibitors could inhibit the Aβ-fibrinogen interaction in the present study [27]. However, our results in Table 1 suggest that Aβ aggregation inhibition itself is not sufficient to inhibit the Aβ-fibrinogen interaction. For example, RS-0406, SEN1576, and tanshinone [36, 41, 42], all of which can strongly inhibit Aβ aggregation and its toxicity, showed negligible efficacy against the Aβ-fibrinogen interaction ($IC_{50} > 100$ μM) (Table 1). In addition, since we used the oligomeric form of Aβ in turbidity assays (Figure 2) and kallikrein activity assays (Figure 5), the ability to inhibit Aβ aggregation, such as these compounds exhibit, may be inconsequential in affecting the result of both assays. Moreover, the duration of both assays (including the incubation time for compound-Aβ mixtures) was less than an hour. It is very unlikely that Aβ aggregation status affects the result of both the assays within an hour, because Aβ fibrillization requires several hours at 37°C (Figure 4A). Therefore, we expect that Aβ binding affinity of compounds could be an important factor in inhibitory efficacy against the Aβ-fibrinogen interaction. In line with this, SEN1269 (5-aryloxypyrimidine) was shown to bind Aβ42 and subsequently block Aβ42's β-pleated sheet assembly and toxicity [32]. Although it is not clear whether SEN1269 or its analog compounds bind directly to fibrinogen, we found that TDI-2760 does not affect normal thrombosis in the turbidity assay (Figure 2D) or blood coagulation in an activated partial thromboplastin time (aPTT) test using human plasma (Figure S2). These results suggest that TDI-2760

does not have any effect on the activity of coagulation proteases. In addition to fibrin polymer formation via coagulation cascade, fibrin(ogen) is also involved in other activities, such as binding to platelets via αIIbβ3 or leukocytes via Mac-1. This type of fibrin(ogen) activity is important for hemostasis or innate immunity [57, 58]. Therefore, to become an effective therapeutic molecule, the influence of TDI-2760 on fibrin(ogen) binding to platelets or leukocytes needs to be examined in future studies.

The contact activation system, driven by FXII, can also launch a proinflammatory pathway that leads to the release of bradykinin upon cleavage of HK [17, 48]. A significantly higher level of HK cleavage is reported in AD patient plasma [17]. Furthermore, it was recently shown that modulating the innate immunity response by knocking out the complement component C3 led to neuroprotection and improved cognitive function in AD mice[59]. These complement C3-knockout AD mice performed better on learning and memory tests despite having more cerebral Aβ deposition. The reduced level of pro-inflammatory markers in these AD mice highlights the important role of inflammation in AD and suggests that targeting the inflammatory pathway could be highly beneficial in treating this disease[59]. Consistent with this finding, our group has shown that reducing neuroinflammation by depleting FXII improves the cognitive function of AD mice [25].

Aβ42 can activate FXII [17, 44-46], which leads to the cleavage of PPK into kallikrein[48]. AD patient plasma has increased levels of kallikrein-like activity compared to that of non-demented control individuals, further suggesting the crucial role of inflammation in AD pathology[17, 19]. TDI-2760 lessens the Aβ42-driven activation of FXII and subsequent release of kallikrein *in vitro* (Figure 5). All these results suggest that TDI-2760 not only alters Aβ42 aggregation but also modulates the other molecular activities of Aβ42, such as fibrinogen interaction and contact system activation. These molecular events are critical in driving vascular and inflammatory pathologies in AD. Therefore, the present study suggests that molecules that can participate in minimizing Aβ42-driven activation of the contact system and can inhibit the Aβ42-fibrinogen interaction would be promising drug candidates for the treatment of AD patients with vascular and inflammatory defects.

Abbreviations:

Aβ, β-amyloid; AD, Alzheimer's disease; aPTT, activated partial thromboplastin time; BSA, bovine serum albumin; CAA, cerebral amyloid angiopathy; CI, confidence interval; DMSO, dimethyl sulfoxide; DXS, dextran sulfate; FXI, coagulation factor XI; FXII, coagulation factor XII; HEPES, 4-(2-hydroxyethyl)-1-piperazineethanesulfonic acid; HFIP, hexafluoro isopropanol; HK, high molecular

weight kininogen; HPLC, high-performance liquid chromatography; IC_{50}, half maximal inhibitory concentration; LHS, left hand side; PPK, plasma prekallikrein; RHS, right-hand side; SAR, structure activity relationship; SEM, scanning electron microscopy; TEM, transmission electron microscopy; ThT; thioflavin T.

Supporting Information: Methods for thrombin activity assay and aPTT test. Supporting Table S1 contains SAR analysis of SEN1269 analogs by LHS modifications. Three supporting figures (S1-S3) show the effect of TDI-2760 on thrombin activity and aPTT, and the effect of SEN1269 on Aβ42 aggregation. This material is available free of charge on the ACS Publications website.

Acknowledgements: This work was supported by the Alzheimer's Drug Discovery Foundation and Robertson Therapeutic Development Fund for HA; NIH grant NS50537, the Tri-Institutional Therapeutics Discovery Institute, Alzheimer's Drug Discovery Foundation, Rudin Family Foundation, and John A. Herrmann for SS. We thank The Rockefeller University's High Throughput, Spectroscopy, and Electron Microscopy Resource Centers for access to experimental equipment and technical support. We thank Zu-Lin Chen and members of Strickland lab for helpful discussion.

Conflict of interest: The authors declare that they have no conflicts of interest with the contents of this article.

Author contributions: PKS performed the experiments, analyzed the results, and wrote the manuscript. MK designed and conducted the chemical synthesis, analyzed the data, and wrote the manuscript. HBR performed the experiments. GN performed the experiments. TY perform the experiments. MAF helped design the experiments, and helped analyze the results. EHN helped analyze the data and wrote the manuscript. SS helped analyze the results and wrote the manuscript. KA designed and performed the chemical synthesis and wrote the manuscript. HJA designed and performed the experiments, analyzed the results, and wrote the manuscript. All the authors edited and approved the final version of the manuscript.

References

(1) Selkoe, D.J. and D. Schenk. (2003) Alzheimer's disease: molecular understanding predicts amyloid-based therapeutics, *Annu Rev Pharmacol Toxicol* 43, 545-584.

(2) Tanzi, R.E. and L. Bertram. (2005) Twenty years of the Alzheimer's disease amyloid hypothesis: a genetic perspective, *Cell* 120, 545-555.

(3) Schmaier, A.H. (2016) Alzheimer disease is in part a thrombohemorrhagic disorder, *J Thromb Haemost* 14, 991-994.

(4) Iqbal, K. and I. Grundke-Iqbal. (2010) Alzheimer's disease, a multifactorial disorder seeking multitherapies, *Alzheimers Dement* 6, 420-424.

(5) Heneka, M.T., M.J. Carson, J. El Khoury, G.E. Landreth, F. Brosseron, D.L. Feinstein, A.H. Jacobs, T. Wyss-Coray, J. Vitorica, R.M. Ransohoff, et al. (2015) Neuroinflammation in Alzheimer's disease, *Lancet Neurol* 14, 388-405.

(6) Mucke, L. and D.J. Selkoe. (2012) Neurotoxicity of amyloid beta-protein: synaptic and network dysfunction, *Cold Spring Harb Perspect Med* 2, a006338.

(7) Haass, C. and D.J. Selkoe. (2007) Soluble protein oligomers in neurodegeneration: lessons from the Alzheimer's amyloid beta-peptide, *Nat Rev Mol Cell Biol* 8, 101-112.

(8) Benilova, I., E. Karran, and B. De Strooper. (2012) The toxic Abeta oligomer and Alzheimer's disease: an emperor in need of clothes, *Nat Neurosci* 15, 349-357.

(9) de la Torre, J.C. (2004) Is Alzheimer's disease a neurodegenerative or a vascular disorder? Data, dogma, and dialectics, *Lancet Neurol* 3, 184-190.

(10) Cortes-Canteli, M., L. Mattei, A.T. Richards, E.H. Norris, and S. Strickland. (2015) Fibrin deposited in the Alzheimer's disease brain promotes neuronal degeneration, *Neurobiol Aging* 36, 608-617.

(11) Serrano-Pozo, A., J. Qian, S.E. Monsell, M.P. Frosch, R.A. Betensky, and B.T. Hyman. (2013) Examination of the clinicopathologic continuum of Alzheimer disease in the autopsy cohort of the National Alzheimer Coordinating Center, *J Neuropathol Exp Neurol* 72, 1182-1192.

(12) Iturria-Medina, Y., R.C. Sotero, P.J. Toussaint, J.M. Mateos-Perez, and A.C. Evans. (2016) Early role of vascular dysregulation on late-onset Alzheimer's disease based on multifactorial data-driven analysis, *Nat Commun* 7, 11934.

(13) Cordonnier, C. and W.M. van der Flier. (2011) Brain microbleeds and Alzheimer's disease: innocent observation or key player?, *Brain* 134, 335-344.

(14) Lee, S., F. Viqar, M.E. Zimmerman, A. Narkhede, G. Tosto, T.L. Benzinger, D.S. Marcus, A.M. Fagan, A. Goate, N.C. Fox, et al. (2016) White matter hyperintensities are a core feature of Alzheimer's disease: Evidence from the dominantly inherited Alzheimer network, *Ann Neurol* 79, 929-939.

(15) Cortes-Canteli, M., J. Paul, E.H. Norris, R. Bronstein, H.J. Ahn, D. Zamolodchikov, S. Bhuvanendran, K.M. Fenz, and S. Strickland. (2010) Fibrinogen and beta-amyloid association alters thrombosis and fibrinolysis: a possible contributing factor to Alzheimer's disease, *Neuron* 66, 695-709.

(16) Zamolodchikov, D., H.E. Berk-Rauch, D.A. Oren, D.S. Stor, P.K. Singh, M. Kawasaki, K. Aso, S. Strickland, and H.J. Ahn. (2016) Biochemical and structural analysis of the interaction between beta-amyloid and fibrinogen, *Blood* 128, 1144-1151.

(17) Zamolodchikov, D., Z.L. Chen, B.A. Conti, T. Renne, and S. Strickland. (2015) Activation of the factor XII-driven contact system in Alzheimer's disease patient and mouse model plasma, *Proc Natl Acad Sci U S A* 112, 4068-4073.

(18) Zamolodchikov, D. and S. Strickland. (2012) Abeta delays fibrin clot lysis by altering fibrin structure and attenuating plasminogen binding to fibrin, *Blood* 119, 3342-3351.

(19) Ashby, E.L., S. Love, and P.G. Kehoe. (2012) Assessment of activation of the plasma kallikrein-kinin system in frontal and temporal cortex in Alzheimer's disease and vascular dementia, *Neurobiol Aging* 33, 1345-1355.

(20) Bergamaschini, L., L. Parnetti, D. Pareyson, S. Canziani, M. Cugno, and A. Agostoni. (1998) Activation of the contact system in cerebrospinal fluid of patients with Alzheimer disease, *Alzheimer Dis Assoc Disord* 12, 102-108.

(21) Brundel, M., J. de Bresser, J.J. van Dillen, L.J. Kappelle, and G.J. Biessels. (2012) Cerebral microinfarcts: a systematic review of neuropathological studies, *J Cereb Blood Flow Metab* 32, 425-436.

(22) Yoshikawa, T., K. Murase, N. Oku, M. Imaizumi, M. Takasawa, P. Rishu, Y. Kimura, Y. Ikejiri, K. Kitagawa, M. Hori, et al. (2003) Heterogeneity of cerebral blood flow in Alzheimer disease and vascular dementia, *AJNR Am J Neuroradiol* 24, 1341-1347.

(23) Cagnin, A., D.J. Brooks, A.M. Kennedy, R.N. Gunn, R. Myers, F.E. Turkheimer, T. Jones, and R.B. Banati. (2001) In-vivo measurement of activated microglia in dementia, *Lancet* 358, 461-467.

(24) Hayes, A., U. Thaker, T. Iwatsubo, S.M. Pickering-Brown, and D.M. Mann. (2002) Pathological relationships between microglial cell activity and tau and amyloid beta protein in patients with Alzheimer's disease, *Neurosci Lett* 331, 171-174.

(25) Chen, Z.L., A.S. Revenko, P. Singh, A.R. MacLeod, E.H. Norris, and S. Strickland. (2017) Depletion of coagulation factor XII ameliorates brain pathology and cognitive impairment in Alzheimer disease mice, *Blood* 129, 2547-2556.

(26) Ahn, H.J., D. Zamolodchikov, M. Cortes-Canteli, E.H. Norris, J.F. Glickman, and S. Strickland. (2010) Alzheimer's disease peptide beta-amyloid interacts with fibrinogen and induces its oligomerization, *Proc Natl Acad Sci U S A* 107, 21812-21817.

(27) Ahn, H.J., J.F. Glickman, K.L. Poon, D. Zamolodchikov, O.C. Jno-Charles, E.H. Norris, and S. Strickland. (2014) A novel Abeta-fibrinogen interaction inhibitor rescues altered thrombosis and cognitive decline in Alzheimer's disease mice, *J Exp Med* 211, 1049-1062.

(28) Cortes-Canteli, M., D. Zamolodchikov, H.J. Ahn, S. Strickland, and E.H. Norris. (2012) Fibrinogen and altered hemostasis in Alzheimer's disease, *J Alzheimers Dis* 32, 599-608.

(29) Ryu, J.K. and J.G. McLarnon. (2009) A leaky blood-brain barrier, fibrinogen infiltration and microglial reactivity in inflamed Alzheimer's disease brain, *J Cell Mol Med* 13, 2911-2925.

(30) Paul, J., S. Strickland, and J.P. Melchor. (2007) Fibrin deposition accelerates neurovascular damage and neuroinflammation in mouse models of Alzheimer's disease, *J Exp Med* 204, 1999-2008.

(31) Klohs, J., C. Baltes, F. Princz-Kranz, D. Ratering, R.M. Nitsch, I. Knuesel, and M. Rudin. (2012) Contrast-enhanced magnetic resonance microangiography reveals remodeling of the cerebral microvasculature in transgenic ArcAbeta mice, *J Neurosci* 32, 1705-1713.

(32) Scopes, D.I., E. O'Hare, R. Jeggo, A.D. Whyment, D. Spanswick, E.M. Kim, J. Gannon, H. Amijee, and J.M. Treherne. (2012) Abeta oligomer toxicity inhibitor protects memory in models of synaptic toxicity, *Br J Pharmacol* 167, 383-392.

(33) Nie, Q., X.G. Du, and M.Y. Geng. (2011) Small molecule inhibitors of amyloid beta peptide aggregation as a potential therapeutic strategy for Alzheimer's disease, *Acta Pharmacol Sin* 32, 545-551.

(34) Stine, W.B., L. Jungbauer, C. Yu, and M.J. LaDu. (2011) Preparing synthetic Abeta in different aggregation states, *Methods Mol Biol* 670, 13-32.

(35) LeVine, H., 3rd. (1999) Quantification of beta-sheet amyloid fibril structures with thioflavin T, *Methods Enzymol* 309, 274-284.

(36) Nakagami, Y., S. Nishimura, T. Murasugi, I. Kaneko, M. Meguro, S. Marumoto, H. Kogen, K. Koyama, and T. Oda. (2002) A novel beta-sheet breaker, RS-0406, reverses amyloid beta-induced cytotoxicity and impairment of long-term potentiation in vitro, *Br J Pharmacol* 137, 676-682.

(37) Wang, H., M.L. Duennwald, B.E. Roberts, L.M. Rozeboom, Y.L. Zhang, A.D. Steele, R. Krishnan, L.J. Su, D. Griffin, S. Mukhopadhyay, et al. (2008) Direct and selective

elimination of specific prions and amyloids by 4,5-dianilinophthalimide and analogs, *Proc Natl Acad Sci U S A* 105, 7159-7164.

(38) Blanchard, B.J., A. Chen, L.M. Rozeboom, K.A. Stafford, P. Weigele, and V.M. Ingram. (2004) Efficient reversal of Alzheimer's disease fibril formation and elimination of neurotoxicity by a small molecule, *Proc Natl Acad Sci U S A* 101, 14326-14332.

(39) Barden, C.J., M.D. Carter, M.A. Reed, D.F. Weaver, A. Yadav, and S. Sun, *Compositions and methods for treating amyloid diseases* in *International Patent WO2010025375 A1*March 4, 2010. p. 151pp.

(40) Byun, J.H., H. Kim, Y. Kim, I. Mook-Jung, D.J. Kim, W.K. Lee, and K.H. Yoo. (2008) Aminostyrylbenzofuran derivatives as potent inhibitors for Abeta fibril formation, *Bioorg Med Chem Lett* 18, 5591-5593.

(41) Wang, Q., X. Yu, K. Patal, R. Hu, S. Chuang, G. Zhang, and J. Zheng. (2013) Tanshinones inhibit amyloid aggregation by amyloid-beta peptide, disaggregate amyloid fibrils, and protect cultured cells, *ACS Chem Neurosci* 4, 1004-1015.

(42) O'Hare, E., D.I. Scopes, E.M. Kim, P. Palmer, D. Spanswick, B. McMahon, H. Amijee, E. Nerou, J.M. Treherne, and R. Jeggo. (2014) Novel 5-aryloxypyrimidine SEN1576 as a candidate for the treatment of Alzheimer's disease, *Int J Neuropsychopharmacol* 17, 117-26.

(43) Hamley, I.W. (2012) The amyloid beta peptide: a chemist's perspective. Role in Alzheimer's and fibrillization, *Chem Rev* 112, 5147-5192.

(44) Maas, C., J.W. Govers-Riemslag, B. Bouma, B. Schiks, B.P. Hazenberg, H.M. Lokhorst, P. Hammarstrom, H. ten Cate, P.G. de Groot, B.N. Bouma, et al. (2008) Misfolded proteins activate factor XII in humans, leading to kallikrein formation without initiating coagulation, *J Clin Invest* 118, 3208-3218.

(45) Shibayama, Y., K. Joseph, Y. Nakazawa, B. Ghebreihiwet, E.I. Peerschke, and A.P. Kaplan. (1999) Zinc-dependent activation of the plasma kinin-forming cascade by aggregated beta amyloid protein, *Clin Immunol* 90, 89-99.

(46) Zamolodchikov, D., T. Renne, and S. Strickland. (2016) The Alzheimer's disease peptide beta-amyloid promotes thrombin generation through activation of coagulation factor XII, *J Thromb Haemost* 14, 995-1007.

(47) Ahn, H.J., Z.L. Chen, D. Zamolodchikov, E.H. Norris, and S. Strickland. (2017) Interactions of beta-amyloid peptide with fibrinogen and coagulation factor XII may contribute to Alzheimer's disease, *Curr Opin Hematol* 24, 427-431.

(48) Renne, T. (2012) The procoagulant and proinflammatory plasma contact system, *Semin Immunopathol* 34, 31-41.

(49) Karran, E., M. Mercken, and B. De Strooper. (2011) The amyloid cascade hypothesis for Alzheimer's disease: an appraisal for the development of therapeutics, *Nat Rev Drug Discov* 10, 698-712.

(50) Ehrnhoefer, D.E., J. Bieschke, A. Boeddrich, M. Herbst, L. Masino, R. Lurz, S. Engemann, A. Pastore, and E.E. Wanker. (2008) EGCG redirects amyloidogenic polypeptides into unstructured, off-pathway oligomers, *Nat Struct Mol Biol* 15, 558-566.

(51) Bieschke, J. (2013) Natural compounds may open new routes to treatment of amyloid diseases, *Neurotherapeutics* 10, 429-439.

(52) Yang, F., G.P. Lim, A.N. Begum, O.J. Ubeda, M.R. Simmons, S.S. Ambegaokar, P.P. Chen, R. Kayed, C.G. Glabe, S.A. Frautschy, et al. (2005) Curcumin inhibits formation of amyloid beta oligomers and fibrils, binds plaques, and reduces amyloid in vivo, *J Biol Chem* 280, 5892-5901.

(53) Habchi, J., S. Chia, R. Limbocker, B. Mannini, M. Ahn, M. Perni, O. Hansson, P. Arosio, J.R. Kumita, P.K. Challa, et al. (2017) Systematic development of small molecules to inhibit

specific microscopic steps of Abeta42 aggregation in Alzheimer's disease, *Proc Natl Acad Sci U S A* 114, E200-E208.

(54) Singh, P.K. and S.K. Maji. (2012) Amyloid-like fibril formation by tachykinin neuropeptides and its relevance to amyloid beta-protein aggregation and toxicity, *Cell Biochem Biophys* 64, 29-44.

(55) Cummings, J.L., T. Morstorf, and K. Zhong. (2014) Alzheimer's disease drug-development pipeline: few candidates, frequent failures, *Alzheimers Res Ther* 6, 37.

(56) Karran, E. and J. Hardy. (2014) A critique of the drug discovery and phase 3 clinical programs targeting the amyloid hypothesis for Alzheimer disease, *Ann Neurol* 76, 185-205.

(57) Weisel, J.W., C. Nagaswami, G. Vilaire, and J.S. Bennett. (1992) Examination of the platelet membrane glycoprotein IIb-IIIa complex and its interaction with fibrinogen and other ligands by electron microscopy, *J Biol Chem* 267, 16637-16643.

(58) Flick, M.J., X. Du, D.P. Witte, M. Jirouskova, D.A. Soloviev, S.J. Busuttil, E.F. Plow, and J.L. Degen. (2004) Leukocyte engagement of fibrin(ogen) via the integrin receptor alphaMbeta2/Mac-1 is critical for host inflammatory response in vivo, *J Clin Invest* 113, 1596-1606.

(59) Shi, Q., S. Chowdhury, R. Ma, K.X. Le, S. Hong, B.J. Caldarone, B. Stevens, and C.A. Lemere. (2017) Complement C3 deficiency protects against neurodegeneration in aged plaque-rich APP/PS1 mice, *Sci Transl Med* 9, aaf6295.

Table 1. Effect of known Aβ aggregation inhibitors on the Aβ42-fibrinogen interaction. Structures and other details of known Aβ aggregation inhibitors/β-sheet breakers used in this study. These compounds were tested for their ability to inhibit the Aβ42-fibrinogen interaction by AlphaLISA. The IC_{50} of these compounds was determined and is presented with the structure of each compound. AlphaLISA shows that Aβ aggregation inhibitors also have an inherent ability to block the Aβ42-fibrinogen interaction; however, the IC_{50} varies substantially among the inhibitors. All AlphaLISA assays were performed in triplicate, and the 95% confidence interval (95% CI) used as a statistical parameter.

Compound (Structure)	Name	Mol. Wt. (Da)	AlphaLISA (IC_{50})	95% CI (μM)
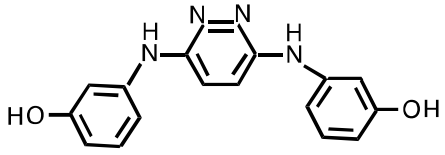	RS-0406	294.31	>100 μM	-
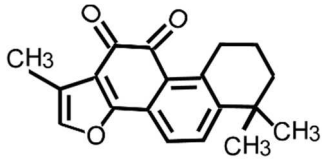	Tanshinone	294.34	>100 μM	-
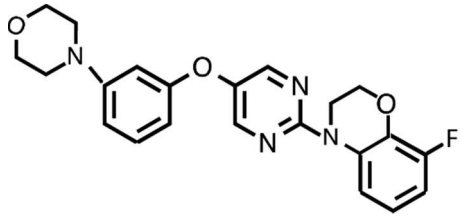	SEN1576	408.43	>100 μM	-
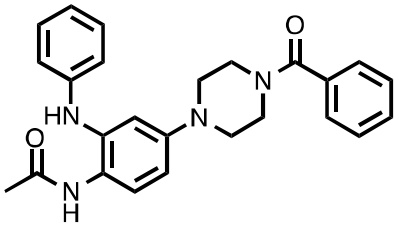	Phenyl amino acetamide derivative	414.51	>100 μM	-
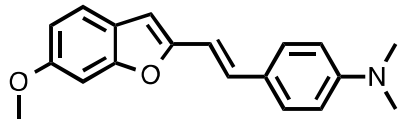	Aminostyryl benzofuran derivative	293.36	49.8 μM	33.2 – 74.8

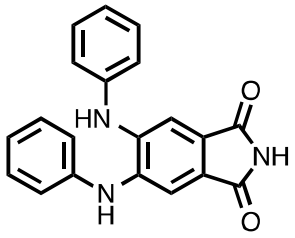	4,5-Dianilino Pthalimide (DAPH)	329.35	43.2 μM	36.4 – 51.4
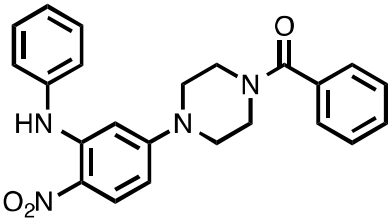	Nitrophenyl piperazinyl derivative	402.45	39.5 μM	25.9 – 60.2
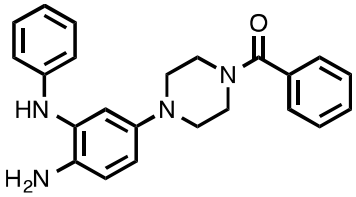	Aminophenyl piperazinyl derivative	372.47	21.0 μM	16.3 – 27.1
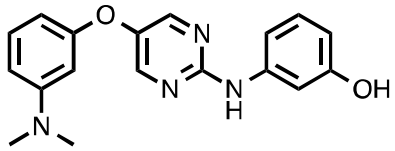	SEN1269	322.36	17.8 μM	16.0 – 19.9

Table 2. Analogs obtained by right-hand side (RHS) modifications of the SEN1269 scaffold. These analogs were tested for their efficacy in blocking the Aβ42-fibrinogen interaction using AlphaLISA. IC_{50} was calculated and compared with that of SEN1269. TDI-2760 (a phenyl analog) showed the lowest IC_{50} among all the compounds tested. All AlphaLISA assays were performed in triplicate, and the 95% confidence interval (95% CI) used as a statistical parameter.

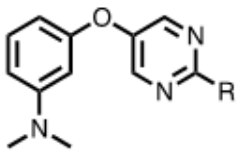

Entry	R	ID	IC_{50} (μM)	95% CI (μM)	Entry	R	ID	IC_{50} (μM)	95% CI (μM)
1	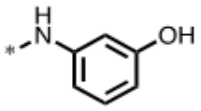	SEN 1269	17.8	16.0 – 19.9	7	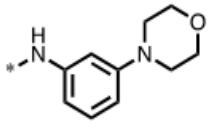	TDI-3099	29.1	24.8-34.2
2	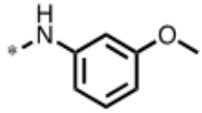	TDI-2758	6.42	5.35 – 7.71	8	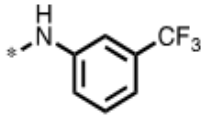	TDI-3071	69.0	60.7 – 78.7
3	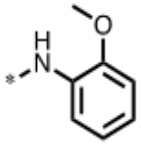	TDI-3066	25.0	19-2 – 32.4	9	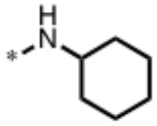	TDI-3078	43.5	39.1 – 48.3
4	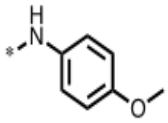	TDI-3067	29.0	24.9 – 34.1	10	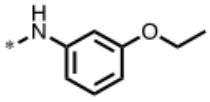	TDI-3277	9.9	7.74 – 12.7
5	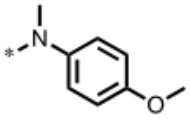	TDI-3082	23.0	18.6 – 28.3	11	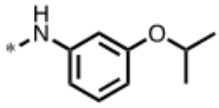	TDI-3275	6.2	3.16 – 12.0
6	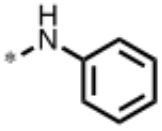	TDI-2760	1.67	1.36 – 2.05					

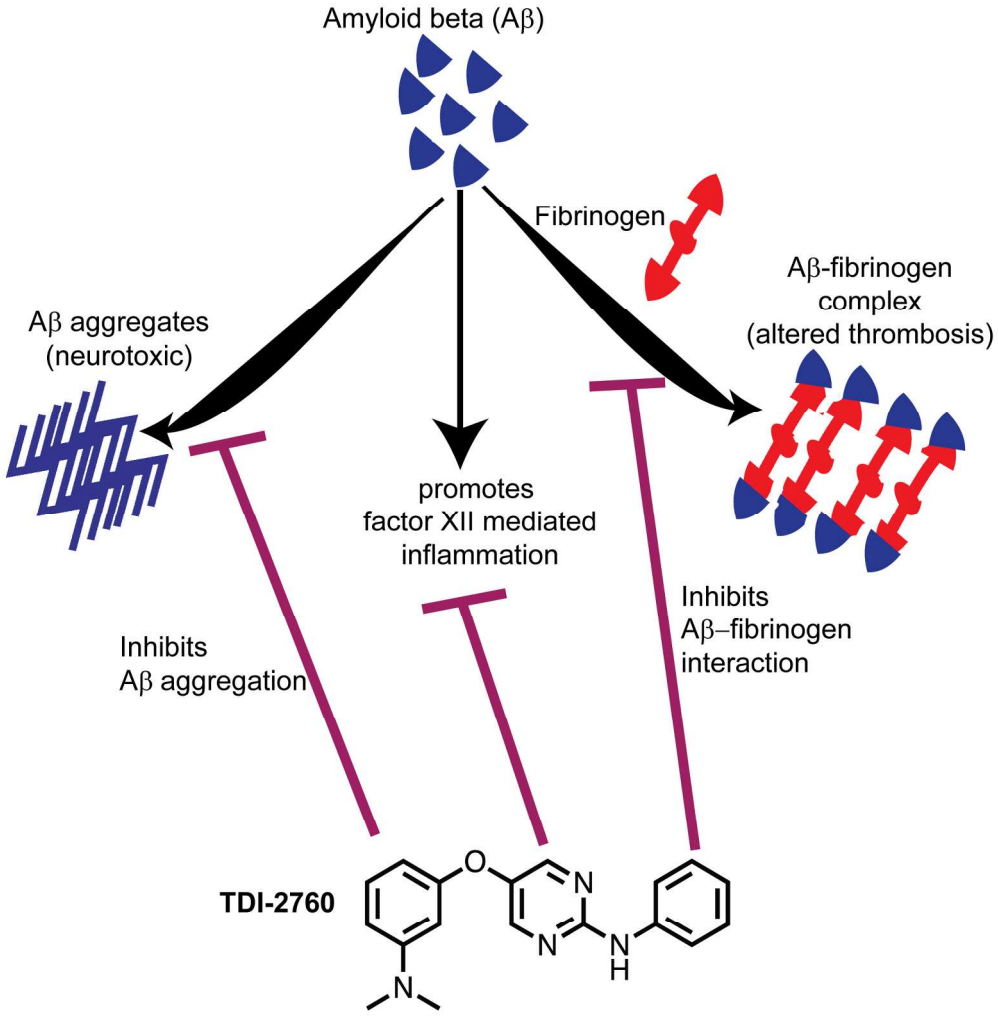

177x181mm (300 x 300 DPI)